Mechanics of Composite Materials, Vol. 48, No. 1, March, 2012 (Russian Original Vol. 48, No. 1, January-February, 2012)

ANALYTICAL PREDICTION OF DAMAGE IN THE COMPOSITE PART OF A TYPE-3 HYDROGEN STORAGE VESSEL

A. Ghouaoula,[1] A. Hocine,[1*] D. Chapelle,[2] F. Karaachira,[3] and M. L. Boubakar[2]

Keywords: *cylindrical vessel, hydrogen, filament winding, liner, analysis of damage behavior*

The damage behavior of a type-3 hydrogen storage vessel is modeled. The vessel consists of a metal envelop, called liner, coated with a filament winding. The model proposed allows simulating the mechanical response of the structure to a quasi-static loading. The model is based on a meso-macro approach and takes into account the damage behavior of the composite and the elastoplastic deformation of the liner. The results obtained are compared with experimental data. Finally, the effect of stacking sequence of filament layers on the damage level in the composite is investigated.

Introduction

Hydrogen is considered as the most promising fuel to solve environmental and energy problems. Fueling vehicles with hydrogen is the core of hydrogen economy and becomes a very interesting topic all over the world. It is not only for protecting the atmosphere from polluting by the emission of toxic gases from conventional vehicles, but also for developing a renewable source of energy [1]. But its storage under highly safe conditions remains an important issue for the introduction of hydrogen in our community, especially for mobile applications as fuel-cell-powered vehicles [2, 3].

Four ways of hydrogen storage are known: (a) in the liquid state, which allows its higher volumetric and gravimetric density, but requires liquefaction of hydrogen gas and an efficiently insulated vessel to reduce its evaporation; (b) in hydrogen storage materials [2], whose main drawback is a smaller gravimetric density compared with that in the case other methods at an identical efficiency; (c) in carbon nanotubes — probably a technology at early development stages; (d) as a compressed gas [4]. The choice of storage type is based on the considerations of high safety, an easy use in terms of energy, density, and

[1]University Hassiba Benbouali BP .151,Chlef 02000, Algeria
[2]Institut FEMTO-ST, Dept. MécAppli, 24, rue de l'épitaphe, 25000 Besançon, France
[3]Sciences and Technology University Oran, Algeria
[*]Corresponding author; tel.: +213 27 72 28 77; fax.: +213 27 72 28 77 ; e-mail: hocinea_dz@yahoo.fr

Russian translation published in Mekhanika Kompozitnykh Materialov, Vol. 48, No. 1, pp. 111-128 , January-February, 2012. Original article submitted October 5, 2011.

dynamics criteria. The hydrogen storage vessel of a fuel-cell-powered vehicle (FCV) should contain 5 kg of hydrogen to be a competitive solution for a 500-km autonomy.

The classification of types of hydrogen pressure storage tanks can be described as follows. Type 1 presents an all-metal cylinder, Type 2 is a load-bearing metal liner hoop-wrapped with a resin-impregnated continuous filament, Type 3 is a non-load-bearing metal liner wrapped in two directions with a resin-impregnated continuous filament, and Type 4 is a non-load-bearing nonmetal liner wrapped in two directions with a resin-impregnated continuous filament. The fiber is generally a carbon one, although, for some peculiar applications, manufacturers may use several layers of glass fiber to reduce costs [5].

The design of a high-pressure hydrogen storage vessel deals with the physical and mechanical properties of materials with regard to its geometry. Before performing a structural optimization, an analysis of behavior of the vessel under an internal pressure is required in order to get a reliable and economical design of composite laminates [6, 7].

The identification of the influence of winding patterns, mechanical properties, and damage mechanisms on the failure behavior of filament-wound pipes requires many experiments, considering various types of loading, such as tension or compression [8, 9] and internal pressure load with different ratios of applied hoop-to-axial stress [10, 11].

Various phenomena have to be mentioned when the damage of a composite is discussed: the transverse cracking of resin, debonding between the fibers and resin, delamination between layers, and fiber breakage. In fact, during the service life of a composite, different damages are going to happen successively and eventually to compete until the final rupture of the material. Lafarie-Frenot et al. [12, 13] studied the cracking of resin in carbon/epoxy composites and quantified the effects of loading amplitude, stacking sequence, and the width of specimens on the development of cracks. They showed that the final density of cracks was strongly associated with the stacking sequence and loading. Joseph and Perreux [14] studied the effect of frequency on the life and damage of filament-wound pipes with $[+55, -55]_n$ laminates under biaxial loading, but this method may be easily generalized to another stackings of type $[+\theta, -\theta]_n$. It was shown that the frequency effect was mainly due to the interaction of creep and fatigue, and the damage development was strongly dependent on the stress ratio. Farines [15] presented an experimental analysis dedicated to the determination of the remaining potential of a tubular composite structure, enabling one to suggest the fatigue design rules.

In the work presented by Hocine at al. [16], an analytical model dedicated to the design of a hydrogen storage vessel is proposes and validated. To do this, six prototypes of tank were manufactured and tested at different pressures. The model allows assessing the mechanical response of the structure. A failure criterion was introduced in order to explore the final static strength of the composite. A following step in this direction could be the account of the damaged composite part, which would make it possible to improve the accuracy of the analytical model.

This work aims to present an evolution of the model and a comparison with experimental results for different stacking sequences.

Mathematical formulation

Let us consider a storage vessel of type 3 consisting of an aluminum liner and a multilayered composite made of a polymer resin reinforced with long fibers (see Fig. 1a). The general stress–strain relationship for each *k*th constituent is given by

$$\begin{Bmatrix} \sigma_z \\ \sigma_\theta \\ \sigma_r \\ \tau_{\theta r} \\ \tau_{zr} \\ \tau_{z\theta} \end{Bmatrix}^{(k)} = \begin{bmatrix} C_{11} & C_{12} & C_{13} & 0 & 0 & C_{16} \\ C_{12} & C_{22} & C_{23} & 0 & 0 & C_{26} \\ C_{13} & C_{23} & C_{33} & 0 & 0 & C_{36} \\ 0 & 0 & 0 & C_{44} & C_{45} & 0 \\ 0 & 0 & 0 & C_{45} & C_{55} & 0 \\ C_{16} & C_{26} & C_{36} & 0 & 0 & C_{66} \end{bmatrix}^{(k)} \begin{Bmatrix} \varepsilon_z \\ \varepsilon_\theta \\ \varepsilon_r \\ \gamma_{\theta r} \\ \gamma_{zr} \\ \gamma_{z\theta} \end{Bmatrix}^{(k)}, \tag{1}$$

where z, θ, and r are cylindrical coordinates.

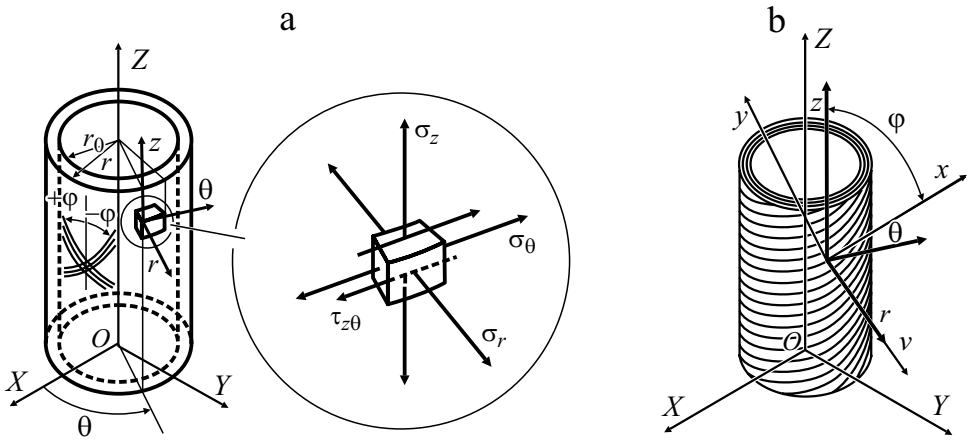

Fig. 1. Composite cylindrical vessel and the stress state in it [16] (a) and the reference and local coordinate systems of the cylindrical vessel (b).

In the particular case of axisymmetric loading, the local equilibrium equation for a *k*th constituent takes the form

$$\frac{d\sigma_r^{(k)}}{dr} + \frac{\sigma_r^{(k)} - \sigma_\theta^{(k)}}{r} = 0, \tag{2}$$

with the radius r of the cylindrical vessel varying in the interval $r_0 \le r \le r_a$, where r_0 and r_a are its inner and outer radii, respectively.

The corresponding strain–displacement relationships are

$$\begin{cases} \varepsilon_r^{(k)} = \dfrac{dU_r^{(k)}}{dr}, \quad \varepsilon_\theta^{(k)} = \dfrac{U_r^{(k)}}{r}, \quad \varepsilon_z^{(k)} = \dfrac{dU_z^{(k)}}{dz} = \varepsilon_0, \\ \gamma_{z\theta}^{(k)} = \dfrac{dU_\theta^{(k)}}{dz} = \gamma_0 r, \quad \gamma_{zr}^{(k)} = 0, \quad \gamma_{\theta r}^{(k)} = \dfrac{dU_\theta^{(k)}}{dr} - \dfrac{U_\theta^{(k)}}{r}. \end{cases} \tag{3}$$

The composite material considered is composed of an organic resin reinforced with long fibers. With respect to the local cylindrical coordinates system (see Fig. 1b), the fourth-order compliance tensor of composite S^c is reduced to the form

$$S^c = \begin{bmatrix} S_{11}^c & S_{12}^c & S_{13}^c & 0 & 0 & 0 \\ S_{12}^c & S_{22}^c & S_{23}^c & 0 & 0 & 0 \\ S_{13}^c & S_{23}^c & S_{33}^c & 0 & 0 & 0 \\ 0 & 0 & 0 & S_{44}^c & S_{45}^c & 0 \\ 0 & 0 & 0 & S_{45}^c & S_{55}^c & 0 \\ 0 & 0 & 0 & 0 & 0 & S_{66}^c \end{bmatrix}$$

with

$$\begin{cases} S_{11}^c = \dfrac{1}{E_{11}},\ S_{12}^c = S_{13}^c = \dfrac{-\nu_{12}}{E_{11}}, \\ S_{22}^c = S_{33}^c = \dfrac{1}{E_{22}},\ S_{23}^c = \dfrac{-\nu_{23}}{E_{22}}, \\ S_{44}^c = \dfrac{1}{G_{12}},\ S_{55}^c = S_{66}^c = \dfrac{1}{G_{23}}, \\ E_{22} = E_{33},\ \nu_{12} = \nu_{13}, \end{cases}$$

where E_{ij} are Young's moduli and ν_{ij} are the Poisson ratios; the 1 and 2, 3 axis are pointed in the longitudinal and transverse directions of the fiber, respectively.

The damage considered in this work is related to the cracking of resin in the direction parallel to fibers. This type of cracking is assumed to change the compliance tensor. In this context, three damage parameters D_{I}, D_{II}, and D_{III} are defined, and they characterize the lower transverse modulus E_{22} and the shear moduli G_{12} and G_{23}.

The damage is introduced by adding the damage contribution tensor H to the compliance tensor of composite S^c [5, 11, 14]. Then, the damaged compliance tensor $\tilde{S}^c$ of a layer takes the form [5]

$$\tilde{S}^c = S^c + H$$

with

$$H = \begin{bmatrix} 0 & 0 & 0 & 0 & 0 & 0 \\ 0 & H_{22}(\sigma,\varepsilon) & 0 & 0 & 0 & 0 \\ 0 & 0 & 0 & 0 & 0 & 0 \\ 0 & 0 & 0 & H_{44}(\sigma,\varepsilon) & 0 & 0 \\ 0 & 0 & 0 & 0 & 0 & 0 \\ 0 & 0 & 0 & 0 & 0 & H_{66}(\sigma,\varepsilon) \end{bmatrix}.$$

The three components H_{22}, H_{44}, and H_{66} of the damage contribution tensor H can be expressed in terms of the three damage parameters to D_{I}, D_{II}, and D_{III} and the components S_{22}, S_{44}, and S_{66} of the compliance tensor of composite S^c:

$$\begin{cases} H_{22} = \dfrac{D_{\mathrm{I}}}{1-D_{\mathrm{I}}} S_{22}, \\ H_{44} = \dfrac{D_{\mathrm{II}}}{1-D_{\mathrm{II}}} S_{44,} \\ H_{66} = \dfrac{D_{\mathrm{III}}}{1-D_{\mathrm{III}}} S_{66}. \end{cases}$$

The only important nonzero components of H are H_{22} and H_{66} (H_{44} has no influence on the present analysis), and the effect of damage on the elastic compliance can be described by using the only damage variable $D_{\mathrm{I}} = \Delta E_2 / E_2$, which means a reduction in the transverse Young's modulus [5]. Therefore, the parameters D_{II} and D_{III} both depend on the only internal variable D_{I}:

$$\begin{cases} D_{\mathrm{II}} = 1 - S_{66}^c \left[S_{66}^c + \dfrac{D_{\mathrm{I}}}{(1-D_{\mathrm{I}})^{1/2}} \left(S_{66}^c S_{22}^c \right)^{1/2} \right]^{-1}, \\ D_{\mathrm{III}} = 1 - S_{44}^c \left[S_{44}^c + \dfrac{D_{\mathrm{I}}}{(1-D_{\mathrm{I}})^{1/2}} S_{22}^c \right]. \end{cases}$$

In the present analysis, only the difference in behavior between the transverse stress and the compression is taken into account. The coefficients H_{44} and H_{66} are assumed to be independent of stress and strain state. The components of the

compliance tensor of the damaged composite can be expressed in terms of the internal variable D_{I} and the sign of the hoop stress:

$$\tilde{S}^c = S^c + H\left(S, D_{\mathrm{I}}, \sigma_2\right),$$

where the damage contribution tensor H is given by

$$H = \begin{bmatrix} 0 & 0 & 0 & 0 & 0 & 0 \\ 0 & H_{22}\, h(\sigma_2) & 0 & 0 & 0 & 0 \\ 0 & 0 & 0 & 0 & 0 & 0 \\ 0 & 0 & 0 & H_{44} & 0 & 0 \\ 0 & 0 & 0 & 0 & 0 & 0 \\ 0 & 0 & 0 & 0 & 0 & H_{66} \end{bmatrix}.$$

If $\sigma_2 < 0$ (crack closure), then $h = 0$; otherwise $h = 1$.

The parameter D_{I} can be calculated from the equation (Appendix A)

$$R^d = \alpha\left(\bar{D}_{\mathrm{I}}\right)^{\beta} = -Y - Y_c,$$

where Y is the driving force of damage and Y_c is the damage threshold.

Considering the liner as an anisotropic elastic material, the fourth-order compliance tensor S_e^L is taken in the form

$$S_e^L = \begin{pmatrix} S_{11}^L & S_{12}^L & S_{13}^L & 0 & 0 & 0 \\ S_{21}^L & S_{22}^L & S_{23}^L & 0 & 0 & 0 \\ S_{31}^L & S_{32}^L & S_{33}^L & 0 & 0 & 0 \\ 0 & 0 & 0 & S_{44}^L & 0 & 0 \\ 0 & 0 & 0 & 0 & S_{55}^L & 0 \\ 0 & 0 & 0 & 0 & 0 & S_{66}^L \end{pmatrix}.$$

Assuming an elastoplastic behavior for the liner, the incremental total strain tensor $d\varepsilon$ is linked to the incremental Cauchy true stress tensor $d\sigma$ as

$$d\varepsilon = d\varepsilon^e + d\varepsilon^p = \left(S_e^L + S_p^L\right) d\sigma,$$

where S_e^L and S_p^L represent the elastic and plastic fourth-order compliance tensors, respectively. The components of S_p^L are given in [16].

Inserting the expressions of radial and hoop stresses derived from Eq. (1) into Eq. (2) and using Eq. (3), the following differential equation is obtained:

$$\frac{d^2U_r^{(k)}}{dr^2} + \frac{1}{r}\cdot\frac{dU_r^{(k)}}{dr} - \frac{N_1^{(k)}}{r^2}U_r^{(k)} = \left[N_2^{(k)}\,\varepsilon_0 + N_3^{(k)}\,\Delta T\right]\frac{1}{r} + N_4^{(k)}\,\gamma_0,$$

where

$$N_1^{(k)} = \frac{C_{22}^{(k)}}{C_{33}^{(k)}}, \quad N_2^{(k)} = \frac{C_{12}^{(k)} - C_{13}^{(k)}}{C_{33}^{(k)}}, \quad N_3^{(k)} = \frac{K_3^{(k)} - K_2^{(k)}}{C_{33}^{(k)}}, \quad N_4^{(k)} = \frac{C_{26}^{(k)} - 2\,C_{36}^{(k)}}{C_{33}^{(k)}},$$

$$\alpha_2^{(k)} = \frac{N_2^{(k)}}{1 - N_1^{(k)}}, \quad \alpha_3^{(k)} = \frac{N_3^{(k)}}{1 - N_1^{(k)}}, \quad \alpha_4^{(k)} = \frac{N_4^{(k)}}{4 - N_1^{(k)}}.$$

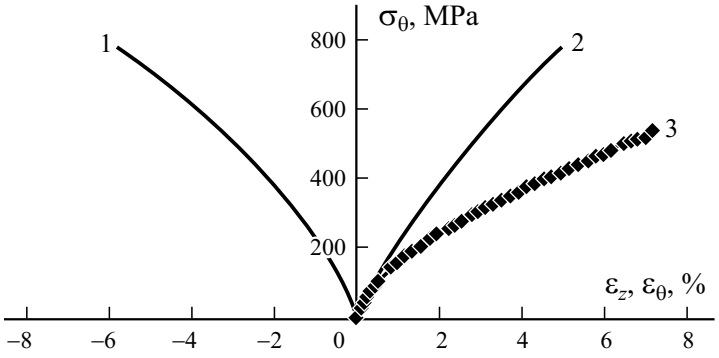

Fig. 2. Analytical (1, 2) and experimental [11] (3) hoop stresses σ_θ as functions of axial ε_z (1) and hoop ε_θ (2, 3) strains in a pressurized composite tube made of a $[\pm 55]_3$ glass/epoxy laminate.

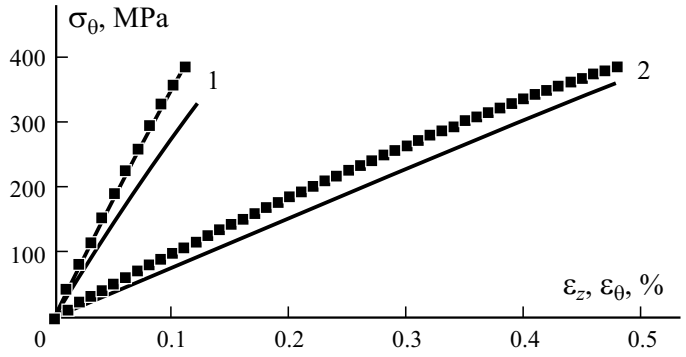

Fig. 3. Analytical (——) and experimental (■) hoop stresses σ_θ as functions of axial ε_z (1) and hoop ε_θ (2) strains in a metallic vessel reinforced with a $[\pm 55]_3$ carbon/epoxy composite.

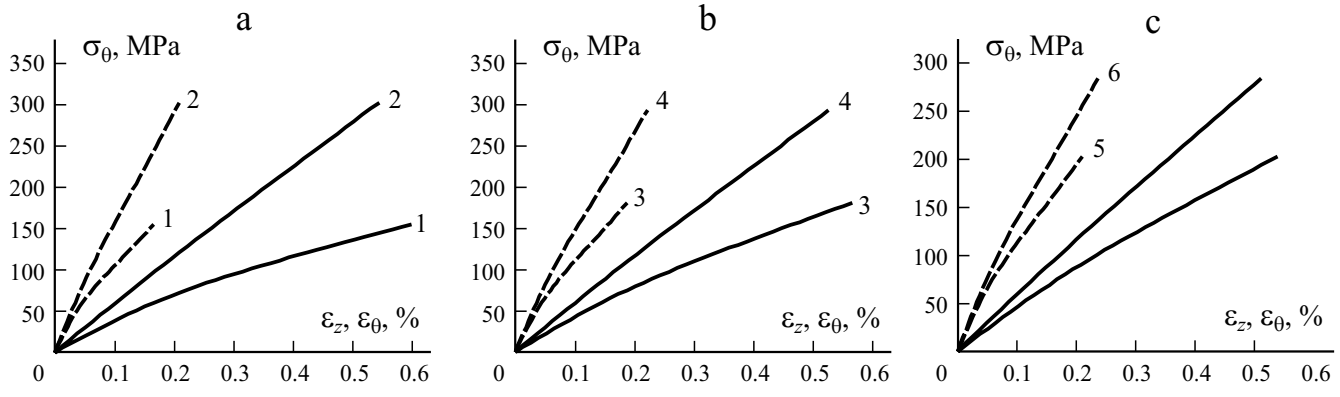

Fig. 4. Hoop stresses σ_θ as functions of axial ε_z (– – –) and hoop ε_θ (——) strains in metallic vessels reinforced with carbon/epoxy composite layers with stacking sequences (numbers at the curves) 1 and 2 (a), 3 and 4 (b), and 5, 6 (c).

The solution of Eq. (4) depends on the value of $\beta^{(k)} = \sqrt{N_1^{(k)}}$.

At $\beta^{(k)} = 1$,

$$U_r^{(k)} = D^{(k)} r + E^{(k)} / r + r \ln(r) \left(N_2^{(k)} \varepsilon_0 + N_3^{(k)} \Delta T \right) + \alpha_4^{(k)} \gamma_0 r^2;$$

at $\beta^{(k)} = 2$,

$$U_r^{(k)} = D^{(k)} r^{\beta^{(k)}} + E^{(k)} r^{-\beta^{(k)}} + \left(\alpha_2^{(k)} \varepsilon_0 + \alpha_3^{(k)} \Delta T \right) r + \frac{N_4^{(k)}}{2} \gamma_0 r^2 \ln(r);$$

at $\beta^{(k)} \neq 1$ (or 2),

$$U_r^{(k)} = D^{(k)} r^{\beta^{(k)}} + E^{(k)} r^{-\beta^{(k)}} + \left(\alpha_2^{(k)} \varepsilon_0 + \alpha_3^{(k)} \Delta T \right) r + \alpha_4^{(k)} \gamma_0 r^2,$$

$D^{(k)}$, $E^{(k)}$, γ_0, and ε_0 being the constants of integration. The superscript k takes values from the interval $[1, w]$, where $w = n_L + n_C + 1$. The constants of integration are calculated by using the boundary conditions given in the appendix B.

A type-3 hydrogen storage tank was submitted to a 40-MPa internal pressure to keep the behavior of the liner purely elastoplastic. The internal radius of the liner was 33 mm, thickness 2 mm, Young's modulus 72 GPa, shear modulus 28.8 GPa, and Poisson ratio 0.25. The thickness of each composite layer was 0.27 mm. The mechanical properties of the glass/epoxy (carbon/epoxy) composite were as follows: E_x = 55 (141.6) GPa, E_y = 21 (10.7) GPa. G_{xy} = 8.267 (3.88) GPa, and v_{xy} = 0.268 (0.268). The solutions were obtained by using the MATLAB numerical code.

Comparison results and validation

1. Composite pipe under internal pressure. Figure 2 presents the analytical and experimental [11] stress–strain curves for a composite glass/epoxy tube made of a $[\pm 55]_3$ laminate and loaded with internal pressure. Both the results points to a loss of stiffness. The pressurized composite pipe showed a circumferential swelling and an axial shrinkage, which did not occur for other schemes of filament winding.

2. Type-3 vessel under internal pressure with an end effect. Figure 3 shows the hoop stress as a function of hoop and axial strains found in experiments and calculated analytically for a metallic vessel reinforced with a $[\pm 55]_3$ carbon/epoxy composite. The plot shows that the agreement between the results from modeling and experiments is rather good.

Figure 4 displays stress–strain curves for the cylindrical part of metallic vessels reinforced by filament windings. Six different stacking sequences of carbon/epoxy layers were investigated: $[\pm 50]_3$ Seq1, $[\pm 50]_2 + [90]_2$ Seq2, $[\pm 55]_3$ Seq3, $[\pm 55]_2 + [90]_2$ Seq4, $[\pm 60]_3$ Seq5, and $[\pm 60]_2 + [90]_2$ Seq6 in order to assess the effect of winding angle on the damage behavior of the composite.

The 90° winding modified the stress/strain distribution across the thickness and decreased the loss of rigidity. In addition, the hoop layer led to a nearly elastic behavior of the vessel. The minimum strains were obtained with the 60° winding angle.

Conclusions

In this work, an analytical model destined for the design of aluminum hydrogen storage vessels wrapped with filament windings is presented and validated. The model is based on a meso-macro approach, which allows one to predict the response of the cylindrical part of a hydrogen storage tank, including the damage behavior of the composite and the elastoplastic deformation of the aluminum liner. In order to clarify the influence of winding patterns on the damage behavior of filament-wound vessels, different stacking sequences of the multilayer composite were investigated.

It was found that, for the stacking sequence $[\pm 55]_3$, the consideration of damage behavior of the composite improved the results of the model, and their agreement with experiments was good. The minimum strains ensured the 60° winding angle.

The reinforcement of the cylindrical part of a vessel by the circumferential winding modified the stress/strain distribution, the response of the vessel became closer to an elastic one, and the loss of its stiffness diminished.

REFERENCES

1. Z. Li, Z. Yaping, and S.Yan, "Enhanced storage of hydrogen at the temperature of liquid nitrogen," Int. J. of Hydrogen Energy, **29**, 319-322 (2004).
2. R. Janot, M. Latroche, and A. Percheron-Guégan, "Development of a hydrogen absorbing layer in the outer shell of high pressure hydrogen tanks," Mater. Sci. and Eng., B, **123**, No. 3, 187-193 (2005).
3. C.-M. Rangel, V.-R. Fernandes, Y. Slavkov, and L. Bozukov, "Integrating hydrogen generation and storage in a novel compact electrochemical system based on metal hydrides," J. of Power Sources, **181**, Nos. 2, 1, 382-385 (2008).
4. Nobuhiko Takeichi, Hiroshi Senoh, Tomoyuki Yokota, Hidekazu Tsuruta, Kenjiro Hamada, Hiroyuki T. Takeshita, Hideaki Tanaka, Tetsu Kiyobayashi, Toshio Takano, and Nobuhiro Kuriyama, "Hybrid hydrogen storage vessel, a novel high pressure hydrogen storage vessel combined with hydrogen storage material," Int. J. of Hydrogen Energy, **28**, 1121-1129 (2003).
5. D. Chapelle and D. Perreux, "Optimal design of a Type 3 hydrogen vessel: Pt I. Analytic modelling of the cylindrical section," Int. J. of Hydrogen Energy, **31**, 627-638 (2006).
6. P. Y. Tabakov and E. B. Summers, "Lay-up optimization of multilayered anisotropic cylinders based on a 3-D elasticity solution," Computers and Structures, **84**, 374–84 (2006).
7. J. Y. Kim, R. Hennig, V. T. Huett, P. C. Gibbons, and K. F. Kelton, "Hydrogen absorption in Ti–Zr–Ni quasicrystals and 1/1 approximants," J. of Alloys and Compounds, **404-406**, 388–391 (2005).
8. J. Bai, P. Seeleuthner, and P. Bompard, "Mechanical behavior of ±55° filament-wound glass-fiber/epoxy-resin tubes: I. Microstructural analysis, mechanical behavior and damage mechanisms of composite tubes under pure tensile loading, pure internal pressure and combined loading," Composites Sci. and Techn., **57**, No. 2, 141-153 (1997).
9. A. A. Smerdov, "A computational study in optimum formulations of optimization problems on laminated cylindrical shells for buckling I. Shells under axial compression," Composites Sci. and Techn., **60**, No. 11, 2057-2066 (2000).
10. J. Rousseau, D. Perreux, and N. Verdière, "The influence of winding patterns on the damage behaviour of filament-wound pipes," Composites Sci. and Techn., **59**, No. 9, 1439-1449 (1999).
11. D. Perreux and F. Thiebaud, "Damaged elasto-plastic behaviour of [+θ,−θ] fibre-reinforced composite laminates in biaxial loading," Composites Sci. and Techn., **54**, No. 3, 275-285 (1995).
12. M. C. Lafarie-Frenot, C. Henaff-Gardin, and D. Gamby, Matrix cracking induced by cyclic ply stresses in composite laminates," Composites Sci. and Techn., **61**, 2327-2336 (2001).
13. D. Gamby, C. Henaff-Gardin, and M. C. Lafarie-Frenot, "Propagation of edge cracking towards the centre of laminated composite plates subjected to fatigue loading," Composite Structures, **56**, 183-190 (2002).
14. D. Perreux and E. Joseph, "The effect of frequency on the fatigue performance of filament-wound pipes under biaxial loading: experimental results and damage model," Composites Sci. and Techn., **57**, 353-364 (1991).
15. L. Farines, Évaluation du potentiel restant de structures composites verre/époxy soumises à des sollicitations de fatigue. Thèse de doctorat. Franche-comté university, Besançon, France. Septembre 2007.
16. A. Hocine, D. Chapelle, L. Boubakar, A. Benamar, and A. Bezazi, "Experimental and analytical of the cylindrical part of a metallic vessel reinforced by filament winding submitted to internal pressure," Int. J. of Pressure Vessels and Piping, **86**, 649-655 (2009).

Appendix A

The function of loading is taken in the form

$$f^d = -Y - Y_C - R^d \leq 0.$$

Then we can write:

$$\dot{D}_1 = 0 \text{ if } f^d < 0 \text{ or } f^d = 0, \ \frac{\partial f^d}{\partial Y}\dot{Y} < 0,$$

$$\dot{D}_1 \neq 0 \text{ if } f^d = 0 \text{ and } \frac{\partial f^d}{\partial Y}\dot{Y} > 0.$$

When loading causes damage,

$$f^d = 0 \quad \text{and} \quad \frac{\partial f^d}{\partial Y}\dot{Y} > 0 .$$

The kinetics of damage is determined by the laws of evolution

$$\dot{D}_{\mathrm{I}} = -\dot{\lambda}^d \frac{\partial f^d}{\partial Y} = \dot{\lambda}^d , \qquad \bar{D}_{\mathrm{I}} = -\dot{\lambda}^d \frac{\partial f^d}{\partial Y} = \dot{\lambda}^d .$$

where $\dot{\lambda}^d$ is the Lagrange multiplier. The expressions can be obtained by using the consistency equation

$$f^d = 0 .$$

We can write

$$R_d = Y_c + Y,$$

$$Y = Y_{\mathrm{I}} + Y_{\mathrm{II}} \times X_{\mathrm{II}} + Y_{\mathrm{III}} \times X_{\mathrm{III}},$$

$$\begin{cases} Y_{\mathrm{I}} = \left[-\dfrac{\partial \psi}{\partial D_{\mathrm{I}}} \right]_{\sigma_4,\sigma_6} = \dfrac{s_{22}}{2\left(1-D_{\mathrm{I}}\right)^2}\sigma_{22}^2, \\ Y_{\mathrm{II}} = \left[-\dfrac{\partial \psi}{\partial D_{\mathrm{II}}} \right]_{\sigma_2,\sigma_4} = \dfrac{s_{66}}{2\left(1-D_{\mathrm{II}}\right)^2}\sigma_{66}^2, \\ Y_{\mathrm{III}} = \left[-\dfrac{\partial \psi}{\partial D_{\mathrm{III}}} \right]_{\sigma_2,\sigma_6} = \dfrac{s_{44}}{2\left(1-D_{\mathrm{III}}\right)^2}\sigma_{44}^2, \\ X_{\mathrm{II}} = \left[-\dfrac{\partial D_{\mathrm{II}}}{\partial D_{\mathrm{I}}} \right] \dfrac{s_{66}\sqrt{s_{11}s_{22}}}{\left(s_{66} + \dfrac{D_{\mathrm{I}}\sqrt{s_{11}s_{22}}}{\sqrt{1-D_I}} \right)^2} \dfrac{\partial}{\partial D_{\mathrm{I}}} \left(\dfrac{D_{\mathrm{I}}}{\sqrt{1-D_{\mathrm{I}}}} \right) = \dfrac{s_{66}\sqrt{s_{11}s_{22}}}{\left(s_{66} + \dfrac{D_{\mathrm{I}}\sqrt{s_{11}s_{22}}}{\sqrt{1-D_{\mathrm{I}}}} \right)^2} \dfrac{2-D_{\mathrm{I}}}{2\left(\sqrt{1-D_{\mathrm{I}}}\right)^3}, \\ X_{\mathrm{III}} = \dfrac{\partial D_{\mathrm{III}}}{\partial D_{\mathrm{I}}} = \dfrac{s_{66}s_{22}}{\left(s_{44} + \dfrac{D_{\mathrm{I}}s_{22}}{\sqrt{1-D_{\mathrm{I}}}} \right)^2} \dfrac{2-D_{\mathrm{I}}}{2\left(\sqrt{1-D_{\mathrm{I}}}\right)^3}. \end{cases}$$

Appendix B

The continuity condition for the radial displacements is

$$\forall\, k \in [1,\, w-1], \quad U^{(k)}\left(r_{\mathrm{ext}}^{(k)}\right) = U^{(k+1)}\left(r_{\mathrm{ext}}^{(k)}\right).$$

The continuity condition for the radial stresses is

$$\begin{cases} \forall\, k \in [1,\, w-1], \quad \sigma_r^{(k)}\left(r_{\mathrm{ext}}^{(k)}\right) = \sigma_{\mathrm{ext}}^{(k+1)}\left(r_{\mathrm{ext}}^{(k)}\right), \\ \sigma_r^{(1)}\left(r_0\right) = -p_0, \\ \sigma_r^{(w)}\left(r_a\right) = 0. \end{cases}$$

The axial equilibrium condition for the solution with the closed-end effect can be expressed as

$$2\pi\sum_{k=1}^{w}\int_{r_{k-1}}^{r_k}\sigma_z^{(k)}(r)\,r\,dr=\pi\,r_0^2\;p_0\;.$$

The zero torsion condition is

$$2\pi\sum_{k=1}^{w}\int_{r^{(k-1)}}^{r^{(k)}}\tau_{z\theta}(r)\,r^2dr=0\;.$$

Finally, the problem can be reduced to a linear system of the form

$$X=A^{-1}\times B\,,$$

$$\begin{bmatrix}D^1\\D^2\\D^3\\D^4\\E^1\\E^2\\E^3\\E^4\\\varepsilon_0\\\gamma_0\end{bmatrix}=\begin{bmatrix}d_{11}&0&0&0&e_{11}&0&0&0&\alpha_{11}&\alpha_{12}\\d_{21}&d_{22}&0&0&e_{21}&e_{22}&0&0&\alpha_{21}&\alpha_{22}\\0&d_{32}&d_{33}&0&0&e_{32}&e_{33}&0&\alpha_{31}&\alpha_{32}\\0&0&d_{43}&d_{44}&0&0&e_{43}&e_{45}&\alpha&\alpha\\d_{15}&d_{52}&0&0&e&e&0&0&\alpha&\alpha\\0&d_{62}&d_{63}&0&0&e&e&0&\alpha&\alpha\\0&0&d_{73}&d_{64}&0&0&e&e&\alpha&\alpha\\0&0&0&d&d&d&e&e&\alpha&\alpha\\d_{91}&d_{92}&d_{93}&d_{94}&e_{91}&e_{92}&e_{93}&e_{94}&\alpha_{91}&\alpha_{92}\\d_{101}&d_{102}&d_{103}&d_{104}&e_{101}&e_{102}&e_{103}&e_{104}&\alpha_{101}&\alpha_{102}\end{bmatrix}^{-1}\times\begin{bmatrix}-P_0\\0\\0\\0\\0\\0\\0\\0\\r_0^2\,P_0/2\\0\end{bmatrix}.$$

The nonzero entries of the quadratic matrix are calculated the boundary conditions given below for $k\in[1,\,w]$, where $w=n_L+n_C+1$.

Internal pressure condition:

$$A_{KK}=C_{23}^K+\beta^K C_{33}^K\left(r^K\right)^{-\beta^K-1},\quad A_{Kn-1}=C_{23}^K+\beta^K C_{33}^K\left(r^K\right)^{-\beta^K-1}.$$

If $\beta^K=1$, else

$$A_{K2n+1}=C_{31}^k+\frac{N_2^K}{2}C_{32}^K\log r^K+C_{33}^K\log r^{K+1},\quad A_{K2n+2}=\left[C_{36}^K+\alpha_2^K\left(C_{32}^K+2C_{33}^K\right)\right]r^K;$$

If $\beta^K\neq1$, else

$$A_{K,2n-1}=\left(C_{23}^K+C_{33}^k\right)\alpha^k+C_{13}^k,\quad A_{K2n+2}=\left[C_{36}^K+\alpha_2^K\left(C_{23}^K+2C_{33}^K\right)\right]r^K.$$

Displacement continuity condition:

$$A_{K,K-1}=\left(r^K\right)^{\beta^{K-1}},\quad A_{K,K}=\left(r^K\right)^{\beta^K},\quad A_{K,K+n-1}=\left(r^K\right)^{-\beta^{K-1}},\quad A_{K,K+n}=\left(r^K\right)^{-\beta^{k1}}.$$

If $\beta^{K-1}=1$ and $\beta^K=1$, then

$$A_{K,2n+1}=R^K\log r^K\,(N_2^{K-1}-N_2^K)/2,\quad A_{K,2n+2}=\left(\alpha_2^{K-1}-\alpha_2^K\right)\left(r^K\right)^2.$$

If $\beta^{K-1}=1$ and $\beta^K\neq1$, then

$$A_{K,2n+1}=R^K\log r^K\left(N_2^{K-1}\right)/2-\alpha_1^K r^K,\quad A_{K,2n+2}=\left(\alpha_2^{K-1}-\alpha_2^K\right)\left(r^K\right)^2.$$

If $\beta^{K-1}\neq1$ and $\beta^K=1$, then

$$A_{K,2n+1}=\alpha_1^K r^K-r^K\lg r^K\frac{N^K}{2},\quad A_{K,2n+2}=\alpha_2^K r^K-\alpha_2^4\left(r^K\right)^2.$$

If $\beta^{K-1}\neq 1$ and $\beta^{K}\neq 1$, then

$$A_{K,2n+1}=\left(\alpha_2^{K-1}-\alpha_1^{K}\right)r^{K},\qquad A_{K,2n+1}=\left(\alpha_2^{K-1}-\alpha_1^{K}\right)\left(r^{K}\right)^2.$$

Strain continuity condition :

$$A_{n+K,K}=\left(C_{23}^{K}+\beta^{K}C_{33}^{K}\right)\left(r^{K+1}\right)^{\beta^{K-1}},\quad A_{n+K,K+1}=\left(C_{23}^{K+1}+\beta^{K+1}C_{33}^{K+1}\right)\left(r^{K+1}\right)^{\beta^{K-1}-1},$$
$$A_{n+K,n+K}=\left(C_{23}^{K}-\beta^{K}C_{33}^{K}\right)\left(r^{K}\right)^{-\beta^{K}-1},\quad A_{n+K,K+n+1}=-\left(C_{23}^{K+1}-\beta^{K+1}C_{33}^{K+1}\right)\left(r^{K+1}\right)^{-\beta^{K-1}-1}.$$

If $\beta^{K}=1$ and $\beta^{K+1}=1$, then

$$A_{n+K,2n+1}=\left[C_{31}^{K}+\frac{N_2^{K}}{2}\left(C_{32}^{K}\log r^{K+1}+C_{33}^{K+1}\left(\log r^{K+1}+1\right)\right)\right]-\left[C_{31}^{K+1}+\frac{N_2^{K}}{2}\left(C_{32}^{K+1}\log r^{K+1}+C_{33}^{K+1}\left(\log r^{K+1}+1\right)\right)\right],$$
$$A_{n+K,K+n+2}=r^{K+1}\left[\left(C_{63}^{K}-C_{63}^{K+1}\right)+\alpha_2^{K}\left(C_{32}^{K}-C_{32}^{K+1}\right)+2\left(C_{33}^{K}-C_{33}^{K+1}\right)\right].$$

If $\beta^{K}=1$ and $\beta^{K+1}\neq 1$

$$A_{n+K,2n+1}=C_{31}^{K}+\frac{N_2^{K}}{2}\left[C_{23}^{K}\log r^{K+1}+C_{33}^{K}\log\left(r^{K+1}+1\right)\right]-\left[C_{13}^{K+1}+\alpha_1^{K}\left(C_{23}^{K+1}+C_{33}^{K+1}\right)\right],$$
$$A_{n+K,K+n+2}=\left\{\left[C_{63}^{K}+\alpha_2^{K}\left(C_{32}^{K}+2C_{33}^{K+1}\right)\right]-\left[C_{63}^{K+1}+\alpha_2^{K+1}\left(C_{32}^{K+1}+2C_{33}^{K+1}\right)\right]\right\}r^{K+1}.$$

If $\beta^{K}\neq 1$ and $\beta^{K+1}=1$, then

$$A_{n+K,2n+1}=C_{13}^{K}+\alpha^{K}\left(C_{23}^{K}+C_{33}^{K}\right)-C_{32}^{K+1}+\frac{N_N^{K+1}}{2}C_{32}^{K+1}\log r^{K+1}+C_{33}^{K+1}\log\left(r^{K+1}+1\right),$$
$$A_{n+K,K+n+2}=\left\{\left[C_{63}^{K}+\alpha_2^{K}\left(C_{32}^{K}+2C_{33}^{K}\right)\right]-\left[C_{63}^{K+1}+\alpha_2^{K+1}\left(C_{32}^{K+1}+2C_{33}^{K+1}\right)\right]\right\}r^{K+1}.$$

If $\beta^{K}\neq 1$ and $\beta^{K+1}\neq 1$, then

$$A_{n+K,2n+2}=C_{13}^{K}-C_{13}^{K+1}+\alpha_1^{K}\left(C_{23}^{K}+C_{33}^{K}\right)-\alpha_1^{K+1}\left(C_{23}^{K+1}+C_{33}^{K+1}\right),$$
$$A_{n+K,2n+2}=\left[\left(C_{36}^{K}-C_{36}^{K+1}\right)+\alpha_2^{K}\left(C_{23}^{K}-2C_{33}^{K}\right)-\alpha_2^{K+1}\left(C_{23}^{K+1}+2C_{33}^{K+1}\right)\right]r^{K+1}.$$

External pressure condition:

$$A_{2n,K}=\left(C_{23}^{n}+\beta^{n}C_{33}^{n}\right)\left(r^{n+1}\right)^{\beta^{n}-1},\qquad A_{2n,2n}=\left(C_{23}^{n}-\beta^{n}C_{33}^{n}\right)\left(r^{n+1}\right)^{\beta^{n}-1},$$
$$A_{2n,2n+1}=C_{13}^{n}+\alpha_1^{n}\left(C_{23}^{n}+C_{33}^{n}\right),\quad A_{2n,2n+2}=\left[C_{36}^{n}+\alpha_1^{n}\left(C_{23}^{n}+C_{33}^{n}\right)\right]r^{n+1}.$$

The axial equilibrium condition:

If $\beta^{K}=1$, then

$$A_{2n+1,K}=\left[\left(r^{K+1}\right)^2+\left(r^{K}\right)^2\right]\frac{C_{12}^{K}+C_{13}^{K}}{2},\quad A_{2n+1,K+n}=\left(\log r^{K+1}-\log r^{K+1}\right)\left(C_{12}^{K}-C_{13}^{K}\right),$$

$$A_{2n+1,K+n}=\sum_{K=1}^{K=n}C_{11}^{K}\frac{\left(r^{K+1}\right)^2}{2}+C_{12}^{K}\frac{N_2}{4}\cdot\frac{1}{2}\left(r^{K+1}\right)^2\left(\log r^{K+1}-\frac{1}{2}\right)+C_{13}^{K}\frac{N_2}{2}\cdot\frac{1}{2}\left(r^{K+1}\right)^2\left[\left(\log r^{k+1}\right)+\frac{1}{2}\right]$$
$$-C_{11}^{K}\left(r^{K+1}\right)^2+C_{12}^{K}\frac{N_2}{2}\left(r^{K}\right)^2\left(\log r^{K}-\frac{1}{4}\right)+C_{13}^{K}\frac{N_2}{2}\cdot\frac{1}{2}\left(r^{K}\right)^2\left[2\log\left(r^{K}\right)^2+\frac{1}{2}\right],$$

$$A_{2n+1,2n+K}=\sum_{k=1}^{k=n}\left[r\left(R^{K+1}\right)^3-\left(R^{K}\right)^3\right]\alpha_2^{K}\left(C_{12}^{K}+2C_{13}^{K}\right)+C_{16}^{K}.$$

If $\beta^{K}\neq 1$, then

$$A_{2n+1,K}=\left(C_{12}^{K}+\beta^{K}C_{13}^{K}\right)\frac{\left(r^{K+1}\right)^{\beta^{K}+1}-\left(r^{K}\right)^{\beta^{K}-1}}{1+\beta^{K}},$$

$$A_{2n+1,K+n}=\left(C_{12}^{K}-\beta^{K}C_{13}^{K}\right)\frac{\left(r^{K+1}\right)^{-\beta^{K}+1}-\left(r^{K}\right)^{-\beta^{K}-1}}{1-\beta^{K}},$$

$$A_{2n+1,2n+1}=\sum_{K=1}^{K=n}\left[C_{11}^{K}+\alpha_{1}^{K}\left(C_{12}^{K}+C_{13}^{K}\right)\right]\frac{\left(r^{K+1}\right)^{2}-\left(r^{K}\right)^{2}}{2},$$

$$A_{2n+1,K+n}=\sum_{K=1}^{k=n}\left(C_{16}^{K}+\alpha_{2}^{K}C_{12}^{K}+2C_{13}^{K}\right)\frac{\left(r^{K+1}\right)^{3}-\left(r^{K}\right)^{3}}{3}.$$

The zero torsion condition:

If $\beta^{K}=1$, then

$$A_{2n+2,K}=\left[\left(r^{K+1}\right)^{3}-\left(r^{K}\right)^{3}\right]\frac{C_{62}^{K}+C_{63}^{K}}{3},\quad A_{2n+2,K+n}=\left(r^{K+1}-r^{K}\right)\left(C_{62}^{K}-C_{63}^{K}\right),$$

$$A_{2n+2,2n+1}=\sum_{k=1}^{k=n}c_{61}^{k}\frac{\left(R^{K+1}\right)^{3}}{3}+\frac{N_{2}^{K}}{2}\cdot\frac{1}{3}\left(r^{K+1}\right)^{3}\left[C_{62}^{K}\left(\log r^{K+1}-\frac{1}{3}\right)+C_{63}^{K}\frac{1}{3}\left(\log r^{K+1}+\frac{2}{3}\right)\right]$$

$$-\left\{C_{61}^{K}\left(r^{K}\right)^{3}+\frac{N_{2}^{K}}{2}\cdot\frac{1}{3}\left(r^{K}\right)^{3}\left[C_{26}^{K}\left(\log r^{K}-\frac{1}{3}\right)+C_{63}^{K}\left(\log r^{K}+\frac{2}{3}\right)\right]\right\},$$

$$A_{2n+2,2n+2}=\sum_{K=1}^{K=n}C_{66}^{K}+\alpha_{2}^{K}\left(C_{62}^{K}+2C_{63}^{K}\right)\frac{\left(R^{K}\right)^{4}-\left(r^{K}\right)^{4}}{4}.$$

If $\beta^{K}\neq 1$, then

$$A_{2n+2,K+n}=\left(C_{26}^{K}+\beta^{K}C_{36}^{K}\right)\frac{\left(r^{K+1}\right)^{\beta^{K}+2}+\left(r^{K}\right)^{\beta^{K}+2}}{2+\beta^{K}},$$

$$A_{2n+2,K+n}=\left(C_{26}^{K}-\beta^{K}C_{36}^{K}\right)\frac{\left(r^{K+1}\right)^{-\beta^{K}+2}+\left(r^{K}\right)^{-\beta^{K}+2}}{2-\beta^{K}},$$

$$A_{2n+2,2n+1}=\sum_{K=1}^{K=n}\left[C_{16}^{K}+\alpha_{1}^{K}\left(C_{26}^{K}+C_{36}^{K}\right)\right]\frac{\left(r^{K+1}\right)^{3}-\left(r^{K}\right)^{3}}{3},$$

$$A_{2n+2,2n+1}=\sum_{K=1}^{K=n}\left[C_{66}^{K}+\alpha_{1}^{K}\left(C_{26}^{K}+2C_{36}^{K}\right)\right]\frac{\left(r^{K+1}\right)^{4}-\left(r^{K}\right)^{4}}{4}.$$

The strains are given by:

If $\beta^{K}\neq 1$, then

$$\varepsilon_{r}^{k}=D^{k}\left(\beta^{k}-1\right)r^{\beta^{k}-1}+E^{k}\left(-\beta^{K}-1\right)r^{-\beta^{k}-1}+\alpha_{2}^{k}\varepsilon_{0}+\frac{N_{4}}{2}\gamma_{0}\left[\frac{1}{3}\left(r^{k}\right)^{3}\ln r-\frac{1}{9}\left(r^{k}\right)^{k}\right],$$

$$\varepsilon_{\theta}^{k}=D^{k}r^{\beta^{k}-1}+E^{k}r^{-\beta^{k}-1}+\alpha_{2}^{k}\varepsilon_{0}+\frac{N_{4}}{2}\gamma_{0}r^{k}\ln r^{k}.$$

If $\beta^{K}=1$, then

$$\varepsilon_{r}^{k}=D^{k}\beta^{k}r^{\beta^{r}-1}+E^{k}\left(-\beta^{k}\right)r^{-\beta^{k}-1}+\alpha_{2}^{k}\varepsilon_{0}+2\alpha_{4}^{k}\gamma_{0}r_{0},$$

$$\varepsilon_{\theta}^{k}=D^{k}r^{\beta^{r}-1}+E^{k}r^{-\beta^{k}-1}+\alpha_{2}^{k}\varepsilon_{0}+\alpha_{4}^{k}\gamma_{0}r_{0}.$$